Neutronics Analysis of the Modular Stellarator Power Reactor UWTOR-M

L. El-Guebaly

May 1983

UWFDM-507

Nucl. Tech./Fusion **4** (1983) 829]. Fusion Energy, 26-28 April 1983, Knoxville, TN.

FUSION TECHNOLOGY INSTITUTE

UNIVERSITY OF WISCONSIN

MADISON WISCONSIN

Neutronics Analysis of the Modular Stellarator Power Reactor UWTOR-M

L. El-Guebaly

Fusion Technology Institute
University of Wisconsin
1500 Engineering Drive
Madison, WI 53706

http://fti.neep.wisc.edu

May 1983

UWFDM-507

Nucl. Tech./Fusion 4 (1983) 829. Fusion Energy, 26-28 April 1983, Knoxville, TN].

DOE/ET52048-28

NEUTRONICS ANALYSIS OF THE MODULAR STELLARATOR POWER REACTOR UWTOR-M

LAILA A. EL-GUEBALY, Nuclear Engineering Department
1500 Johnson Drive, University of Wisconsin
Madison, WI 53706
(608) 262-4854

ABSTRACT

Neutronics and photonics analysis for UWTOR-M was carried out to assess radiation streaming effects on reactor performance. The effect the lithium enrichment in the $Li_{17}Pb_{83}$ breeder has on radiation streaming was investigated. Using an enrichment of 35% was found to yield an adequate tritium breeding ratio of 1.08 and an overall energy multiplication of 1.153. The bulk shield was optimized to reduce the radiation effects in the superconducting magnets with the limited shielding space available in the design. Detailed analysis for the radiation streaming into the divertor regions has been performed. The divertor targets were found to recover 91% of the streaming energy.

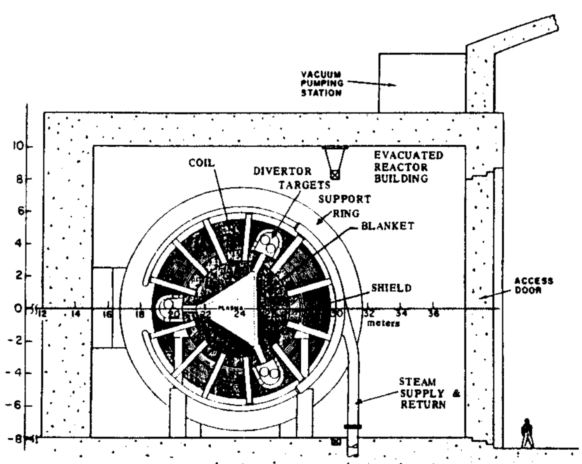

Fig. 1. Vertical cross section of the UWTOR-M reactor.

INTRODUCTION

Radiation streaming through penetrations in fusion reactors has significant impact on important reactor parameters such as tritium breeding ratio (BR) and energy multiplication (M). Although the stellarator is one of the earliest proposed magnetic confinement concepts,[1] it was only in the past three years that interest in stellarators has been revived as a result of recent encouraging experimental results.[2] The UWTOR-M[3] modular stellarator power reactor design utilizes large divertor penetrations for impurity control. A vertical cross section showing the main features of the reactor is given as Fig. 1. The breeding blanket consists of three segments with different cross-sectional areas. The radial neutron source density distribution peaks at the center of the triangular plasma zone. The total neutron source rate is 1.52×10^{21} n/s which corresponds to a fusion power of 4297 MW (at 17.6 MeV/fusion). Some neutrons and gamma photons will stream through the three divertor slots which occupy ~ 5% of the solid angle. Therefore, shielding materials are used in the divertor targets to protect vital components in the toroidal hall and to recover part of the energy carried by streaming radiation.

The blanket was designed to achieve the largest energy multiplication with adequate tritium breeding. The effect the Li enrichment has on radiation streaming was investigated. The magnet shield optimization was performed to design a shield which provides adequate protection for the superconducting (s/c) magnet utilizing the limited shielding space available. The radiation streaming problem was analyzed and the calculational features of this problem are presented in the last section.

BLANKET NEUTRONICS ANALYSIS

The primary goal of this analysis is to achieve an overall tritium breeding ratio greater than one with the largest energy multiplication. The blanket and its associated shield can be represented approximately by the schematic shown in Fig. 2. The average thickness of the three different blanket segments is 1.154 m. The $Li_{17}Pb_{83}$ breeder[4] is cooled by 9 vol% steam and the ferritic steel HT-9 is the structural material in the blanket. The presence of the back structural ribs yields an increase in the structure content in the last 0.3 m of the blanket. Other features include the use of Fe-1422 steel in the 0.4 m thick reflector to enhance the energy multiplication by intercepting most of the neutron and gamma energies before leaking into the shield.

The schematic shown in Fig. 2 was modeled in the one-dimensional (1-D) calculations to give only a qualitative feel for the effects of any changes in the enrichment and structure content on the BR and M. These calculations were carried out using the 1-D discrete ordinates code ONEDANT,[5] the standard Los Alamos data with coupled 30 neutron and 12 gamma energy groups, and the P_3-S_8 approximation, in cylindrical geometry. The cross section data used are based on ENDF/B-V evaluation.

Calculations have been performed in which the lithium enrichment and structure content were varied. A plot of the local BR versus M for the various cases is represented in Fig. 3. An inspection of this figure shows that decreasing the enrichment results in decreasing BR and increasing M. This is due to the fact that reducing the ^6Li percentage in lithium gives more chance for neutrons to be parasitically absorbed in the structural material with the subsequent release of more energy. Also, decreasing the enrichment results in larger increases in M than does increasing the structure content. Furthermore, increasing the structure content results in an appreciable reduction in BR since an amount of the breeding material is replaced by structure. Figure 3 reveals that, for a fixed blanket thickness, the best way to increase M without having a drastic reduction in BR is to lower the enrichment and keep the structure content to its minimum value.

Three-dimensional (3-D) calculations were performed using MCNP[6] and the results are based on 5,000 histories yielding relative standard deviations of less than 2% for the quantities of interest. A view emphasizing the blanket is shown in Fig. 4 which is an output from the plotting routine of MCNP. The structure content in the blanket was kept at 9 vol% and the enrichment was varied gradually between 20 and 40%. The effect the enrichment has on radiation streaming is indicated in Fig. 5. The fraction of primary neutrons streaming is less than that indicated by the solid angle fraction of the divertor slots (5%) because source neutrons are distributed in the triangular plasma zone. A fraction of 5% would have streamed if all source

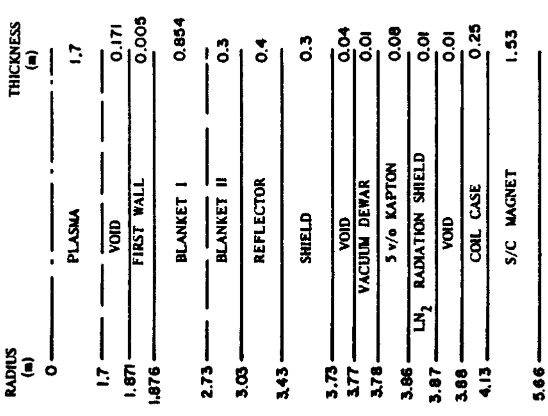

Fig. 2. Schematic of blanket, reflector, shield, and s/c magnet.

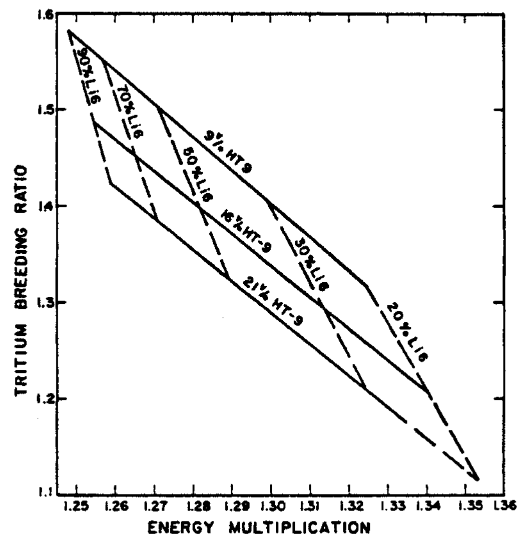

Fig. 3. Variation of tritium breeding ratio with energy multiplication for different ^6Li enrichment and structure contents.

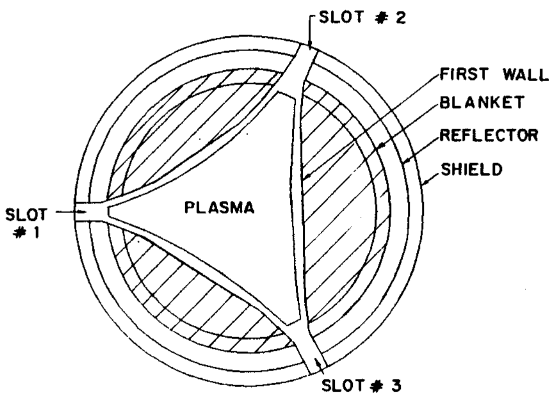

Fig. 4. Blanket and shield geometrical model used for 3-D calculations.

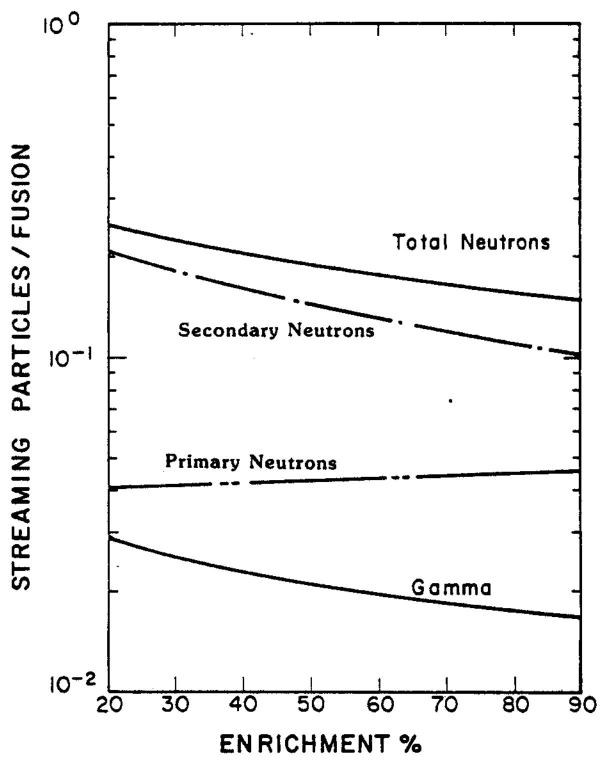

Fig. 5. Effect of ^6Li enrichment on radiation streaming into the divertor regions.

neutrons were emitted at the plasma centerline. The streaming of primary neutrons increases slightly with enrichment due to the decreased blanket attenuation for the 14 MeV neutrons as a result of the lower ^7Li content. However, the opposite effect is obtained for the secondary neutrons due to the increased attenuation by ^6Li. The gamma generation in the blanket structure decreases as the enrichment increases resulting in less gamma streaming.

The 3-D results show that an enrichment of 35% gives an adequate overall tritium breeding ratio of 1.08 and an energy multiplication of 1.153 (M is defined as the nuclear heating in the first wall, blanket, reflector, and the six divertor targets per 14.1 MeV source neutron). More than 98% of the breeding is contributed from ^6Li and, as expected, blanket I breeds most of the tritium. About 54% of the total nuclear heating results from gamma heating. The overall BR and M are, as anticipated, lower than the local values due to radiation streaming. In addition, the thin blanket regions surrounding the divertor slots result in larger neutron and gamma ray leakage to the reflector and bulk shield.

BULK SHIELD OPTIMIZATION

Several 1-D calculations were carried out to determine the optimum shield composition which provides adequate protection for the superconducting magnets. The magnet radiation limits are set by several criteria: deterioration of thermal and electrical insulators, the cryogenic heat load, and the resistivity increase in the copper stabilizer. Epoxy is used for electrical insulation while aluminized Kapton, which has been found to be ~ 100 times more radiation resistant than aluminized Mylar,[7] is used as thermal insulator. Dose limits for epoxy and Kapton are taken as 5×10^8 and 10^{10} rads, respectively. These insulators must last for the whole reactor life estimated to be 24 full power years (FPY) (based on 80% availability). The limit on the peak heat load in the s/c magnet is considered to be 0.06 mW/cm^3. The superconducting magnet design requires that the displacement per atom (dpa) in the Cu stabilizer does not exceed 1.6×10^{-4} dpa. Once this value of dpa is reached, the magnet must be annealed to ensure proper performance.

The space available for the shield is only 0.3 m. An attempt was made to heterogenize the shield to efficiently utilize the shielding capability of the materials. The steel layer (95 vol% Fe-1422 and 5 vol% H_2O), which is effective in slowing down the high energy neutrons, is placed in front of the B_4C layer (86 vol% B_4C (87% d.f.), 10 vol% Fe-1422, and 4 vol% H_2O), which moderates the neutrons further and acts as a good absorber for low energy neutrons. A thin layer of lead is placed at the back of the shield to attenuate the generated gamma rays. In the poloidal direction of the reactor, the position of the magnet varies behind the blanket segments. Parts of the magnet that are behind the middle of the segments are overprotected by the relatively thick blanket. The worst radiation effects occur in portions of the magnet behind the 0.4 m diameter steam headers (located close to the divertor entrance) where only ~ 0.5 m of blanket thickness is available in the smallest blanket segment. To assess the peak radiation damage in the magnet, the geometrical configuration at the steam headers was modeled in the 1-D calculations.

The radiation dose in the superinsulator in front of the magnet was found to be the design driver for the shield as other magnet components are further protected by the 0.25 m coil case. A series of 1-D calculations was carried out in which the thicknesses of the three shield layers were varied one at a time to determine the optimum shield configuration. In the first set of calculations, the thickness of the lead layer was varied with the thicknesses of the steel layer relative to the B_4C layer kept the same. The results indicate that 0.043 m of lead layer is required to minimize the total dose in Kapton. In the second set of calculations, the thickness of the lead layer was kept fixed at 0.043 m, while the B_4C layer was increased under the constraint that the total shield thickness remains 0.3 m. The optimization study reveals that a substantial amount of B_4C is required for radiation attenuation. This is due to the fact that the energy spectrum behind the LiPb blanket and metallic reflector is considerably soft and B_4C is more suitable for attenuating such spectra than steel. To satisfy the design criteria for Kapton, the thickness of the B_4C layer was set at 0.2 m which yields 8.757 x 10^9 rads/24 FPY in Kapton. Other data of interest are the peak dpa in the Cu stabilizer, the peak power density in the magnet, and the peak dose in epoxy. These are 6.476 x 10^{-6} dpa/FPY, 0.016 mW/cm^3, and 4.163 x 10^8 rads/24 FPY, respectively. The dpa rate implies that magnet annealing is not required during the whole reactor life.

RADIATION STREAMING ANALYSIS

Radiation streaming through the divertor slots and pumpout ports has large impact on the operation and maintenance of the reactor and its sensitive equipment. The effectiveness of the bulk shield is reduced by the streaming of radiation through the slots. Thus, the divertor regions are also required to be shielded. Three-dimensional neutronics and photonics calculations were performed using the MCNP code. The calculational procedure was divided into two parts by modeling the geometrical configuration of the reactor in two separate problems. The blanket and shield shown in Fig. 4 is considered as one problem and the divertor targets and associated shield shown in Fig. 6 is the other.

Radiation Streaming Through Divertor Slots

Trapping surfaces were located at the entrance of the three divertor regions of Fig. 4. At these surfaces all particles entering the divertor regions are counted according to angle and energy bins. This information was then stored to serve as a surface source in later modeling of the divertor region itself. A run of 5,000 histories was sampled isotropically from the spatial variation of the source within the triangular plasma zone. The relative standard deviations were less than 6% for the quantities of interest. The results show that for each D-T fusion event, the total neutrons and gamma photons streaming through the three divertor slots are 0.214 and 0.024, respectively, carrying a total energy of 0.723 MeV. The total power carried by streaming radiation is 176 MW which represents 5% of the neutron fusion power and fortunately most of it is recovered by the divertor targets as will be shown later. Detailed results of particles crossing the different trapping surfaces are given in Table I on a per fusion and per second basis along with the energy carried by streaming radiation. Tabulated results show that the amounts of streaming radiation differ slightly for each slot depend-

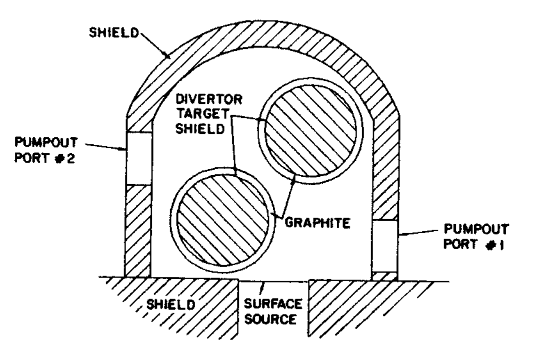

Fig. 6. Geometrical model of divertor region.

ing on the size of the blanket segment surrounding it. Also, 83% of the energy is carried by the primary streaming neutrons. The average energies of the streaming neutrons and gamma photons are 3.229 and 1.332 MeV, respectively. The angular distributions peak at normal incidence and most particles will go into the divertor targets.

Divertor Region Model

A run of 30,000 histories was performed for the divertor region problem employing neutron and gamma surface sources at the entrance of 7.122×10^{-2} and 8.096×10^{-3} particles/fusion, respectively, as obtained from the previous run. The purpose of the calculations was twofold: (a) to obtain information about radiation exiting each pumpout port through the use of trapping surfaces, and (b) to estimate the amount of energy recovered by the divertor targets.

The divertor region was modeled for the Monte Carlo code MCNP and Fig. 6 is an output from its plotting routine. The pair of rotating divertor targets are made of Fe-1422 steel, cooled with 10% steam by volume and covered with several centimeters of graphite. Charged particles striking these targets are neutralized and scattered into zones from which they are pumped out through the ports. The pumpout ports are located appreciably off the direct line of sight of the flowing particles from the divertor region entrance. This is of importance in reducing radiation streaming through the ports.

The results indicate that considerable attenuation and spectrum softening result from neutron interactions with divertor targets. The average energies of streaming neutrons through ports #1 and 2, which are 0.913 and 0.362 MeV, respectively, are significantly softer than the corresponding 3.229 MeV of the streaming neutrons at the entrance to the divertor region. The neutron spectrum at port #1 contains a few high energy neutrons, as expected, since the port is not directly in line with the plasma neutrons. Also, most of the neutrons can stream out of the port only through multiple scattering collisions with the divertor targets that degrade their energies considerably. These effects are more pronounced for streaming neutrons through port #2. About 80% of the streaming gamma rays are from those generated in the divertor targets resulting from parasitic neutron absorption in the steel. Their average energies are slightly smaller than those of gamma photons entering the divertor region. The total power carried by radiation streaming through all ports of the three divertor regions is 6.12 MW representing only 0.178% of the neutron fusion power. Most of the particles entering the divertor region deposit their energy in the divertor targets as evidenced by the fact that the nuclear heating per each pair of targets is 0.218 MeV/fusion of which 81% is gamma heating. This corresponds to 91% of the energy carried by radiation streaming into the divertor region from the reaction chamber.

TABLE I. Radiation Streaming Through Divertor Slots

Slot #	Neutron						Gamma	
	Primary		Secondary		Total		Per Fusion	Per Sec
	Per Fusion	Per Sec	Per Fusion	Per Sec	Per Fusion	Per Sec		
1	1.530E-2	2.326E19	6.084E-2	9.248E19	7.614E-2	1.157E20	8.628E-3	1.312E19
2	1.435E-2	2.181E19	6.297E-2	9.571E19	7.732E-2	1.175E20	8.735E-3	1.328E19
3	1.199E-2	1.823E19	4.819E-2	7.325E19	6.018E-2	9.147E19	6.924E-3	1.052E19
Total into 3 slots	4.164E-2	6.330E19	0.172	2.614E20	0.214	3.247E20	2.429E-2	3.692E19
Streaming Energy (MeV/Fusion)	0.576		0.114		0.690		0.033	

Due to the necessity of penetrations in the bulk shield, radiation streaming raises the biological dose levels. Comparison between the radiation current outside the bulk shield and that at the pumpout port #1 shows that the latter is at least factors of 50 and 100 higher for neutrons and gamma rays, respectively. On this basis, the information obtained from the divertor model was used to define a plane source for the subsequent 1-D calculations to estimate the required concrete shield thickness. The peak biological dose rate occurs at parts outside the inboard concrete shield closest to the divertor region. A 3.1 m thick biological shield was found to result in an acceptable dose of 2.35 mrem/h in the toroidal service hall during reactor operation.

SUMMARY

The effects of radiation streaming through the divertor slots and pumpout ports have been evaluated. Although 21% of the neutrons stream through the divertor slots, a tritium breeding ratio of 1.08 and energy multiplication of 1.153 were achieved using 35% enriched lithium in the $Li_{17}Pb_{83}$ breeder and structure content of 9 vol% HT-9 in the blanket. A thick reflector made of Fe-1422 steel was used to enhance the energy multiplication. The bulk shield composition was optimized to reduce the radiation damage and heat load in the superconducting magnets. This results in an acceptable dose in Kapton and epoxy insulators after the estimated 24 FPY's reactor life. In addition, no magnet annealing is required during the whole reactor life.

Only 20% of the radiation streaming through the divertor slots are primary neutrons and they carry 83% of the streaming energy. Considerable attenuation and spectrum softening result from neutron interactions with divertor targets which, as a result, recover 91% of the energy streaming into the divertor regions. A 3.1 m thick concrete shield is required to maintain an acceptable biological dose during operation in the toroidal service hall.

One major conclusion is that despite the large radiation streaming through the divertor slots in a stellarator reactor, proper choice of blanket materials and composition can provide an adequate tritium breeding ratio and energy multiplication. In addition, high performance divertor targets can be used to intercept and recover most of the streaming radiation energy.

ACKNOWLEDGMENT

This work was funded by the U.S. Department of Energy.

REFERENCES

1. B. BADGER et al., "UWTOR-M, A Conceptual Modular Stellarator Power Reactor," UWFDM-550, Fusion Engineering Program and Torsatron/Stellarator Lab., University of Wisconsin (1982).

2. L. SPITZER et al., "Problems of the Stellarator as a Useful Power Source," USAEC Report NYO-6047 (1954).

3. G. CATTANEI et al., "Neutral Injection Heating in the Wendelstein VII-A Stellarator," 9th International Conference on Plasma Physics and Controlled Nuclear Fusion Research IAEA-CN-41, Baltimore, MD, USA, Sept. (1982).

4. D.K. SZE et al., "LiPb, A Novel Material for Fusion Applications," Proc. Fourth ANS Topical Meeting on the Technology of Controlled Nuclear Fusion (1980).

5. R.D. O'DELL et al., "User's Manual for ONEDANT: A Code Package for One-Dimensional, Diffusion-Accelerated, Neutral-Particle Transport," Los Alamos National Laboratory LA-9184-M (1982).

6. Los Alamos Monte Carlo Group X-6, "MCNP - A General Monte Carlo Code for Neutron and Photon Transport, Version 2C," LA-7396-M, Revised (1981).

7. C. LONG et al., "Effects of Radiation at 5 K on Organic Insulators for Superconducting Magnets," Special Purpose Materials Annual Progress Report, U.S. Dept. of Energy Report DOE/ER-0048/1, pp. 73-88 (1980).